Nanoscale



COMMUNICATION

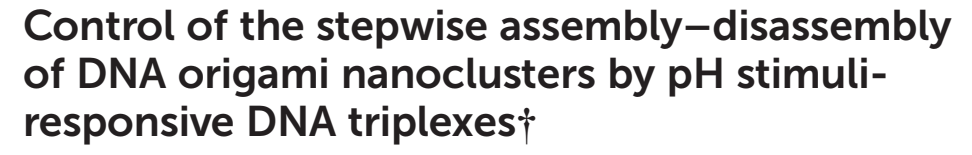
View Article Online
View Journal | View Issue



Cite this: Nanoscale, 2019, 11, 18026

Received 13th June 2019, Accepted 22nd September 2019 DOI: 10.1039/c9nr05047q

rsc.li/nanoscale



Shuo Yang, a Wenyan Liua, b and Risheng Wang ** **

We present the pH-triggered reversible assembly of DNA origami clusters in a stepwise fashion. The structure formation and dissociation are controlled by a series of consecutive pH-stimulation processes that rely on the triplex-to-duplex transition of DNA triplexes in different pH conditions. This multilevel dynamic assembly strategy brings more structural complexity and provides the possibility of developing intelligent materials for engineering applications.

Living systems represent the most efficient and adaptable example of the stepwise assembly of functional macromolecules in response to external and internal stimuli and, in some cases, these assemblies can also disassemble into their individual components when triggered by other signals. For example, the stepwise assembly of multiple protein subunits into DNA polymerase III holoenzyme, under successive physiological stimuli, is a key to ensure that DNA replicates in high fidelity and high processivity.2 In view of the sophisticated self-assembly process and intriguing functional abilities of biological systems, the mimicking of their stimuli-responsive reversible assembly/disassembly behavior, through use of synthetic biomolecules, has proven to be one of the most promising, yet challenging aspects of nanoscience. Benefited by its superior programmability (as per Watson-Crick base paring), DNA has been widely utilized for the self-assembly of a diversity of pre-designed 2D and 3D DNA nanostructures. 3-12 This makes DNA a well-suited candidate for creating dynamic reconfigurable assembly systems. 13-16 The self-assembly of stimuli-responsive DNA architectures, in a stepwise fashion, could endow conventional static DNA structures with defined

Recently, extensive research efforts have been devoted to exploring the reversible multimerization of DNA origami nanostructures in response to various external stimuli. 17-25 Examples include the reversible assembly of hexagon-shaped DNA origami controlled by photoirradiation between UV and visible light, 17 and the K+-ion stimulated assembly of DNA origami dimers by use of G-quadruplexes.21,25 Recently, the reconfiguration of DNA origami dimers and trimers have been achieved based on pH-sensitive i-motif, and triplex DNA, 18 in which the DNA origami trimers assembled under neutral conditions could transit into a mixture of dimers and monomers when the assemblies were subjected to either acidic or basic conditions. Those pioneering studies on the dynamic assembly of DNA structures in response to a single-step stimulus between a two-state transition have inspired us to design a consecutive multi-step transition system, which was induced by multiple steps of environmental stimulation that is able to reversibly and selectively create complicated and larger DNA nanostructures (>5 units). The realization of such a dynamic and elegant fabrication process will extend our capabilities to synthesize intelligent biomaterials with well-defined structures, which represent one step forward towards the imitation of designs and processes that are found in nature.

In this study, we present the pH-regulated, multistep cyclic self-assembly of DNA origami nanoclusters by employing DNA triplexes as dynamic linkers (Fig. 1). The DNA triplex is formed by the interaction between a pH-insensitive Watson–Crick duplex and a single-stranded DNA (ssDNA) through pH-sensitive parallel Hoogsteen base-pairing. The triplex-to-duplex (closing-to-opening) transition is strongly pH dependent, and its pH sensitivity can be regulated by manipulating the ratio of C-G·C vs. T-A·T in the DNA sequence because C-G·C triplets prefer acidic pH and T-A·T triplets favor a neutral pH. As such, it is possible to allow the triplex-to-duplex transition to take place in a desired pH range. In an opening state, the

geometry, and novel capabilities in sensing, monitoring, and dynamic controls in the areas of nanodevices, matematerials, and nanomedicine.

^aDepartment of Chemistry, Missouri University of Science and Technology, Rolla, MO 65409, USA. E-mail: wangri@mst.edu

^bCenter for Research in Energy and Environment, Missouri University of Science and Technology, Rolla, MO 65409, USA

[†]Electronic supplementary information (ESI) available: Detailed experimental procedures, AFM images, gel electrophoresis images and DNA sequences. See DOI: 10.1039/c9nr05047g

Nanoscale Communication

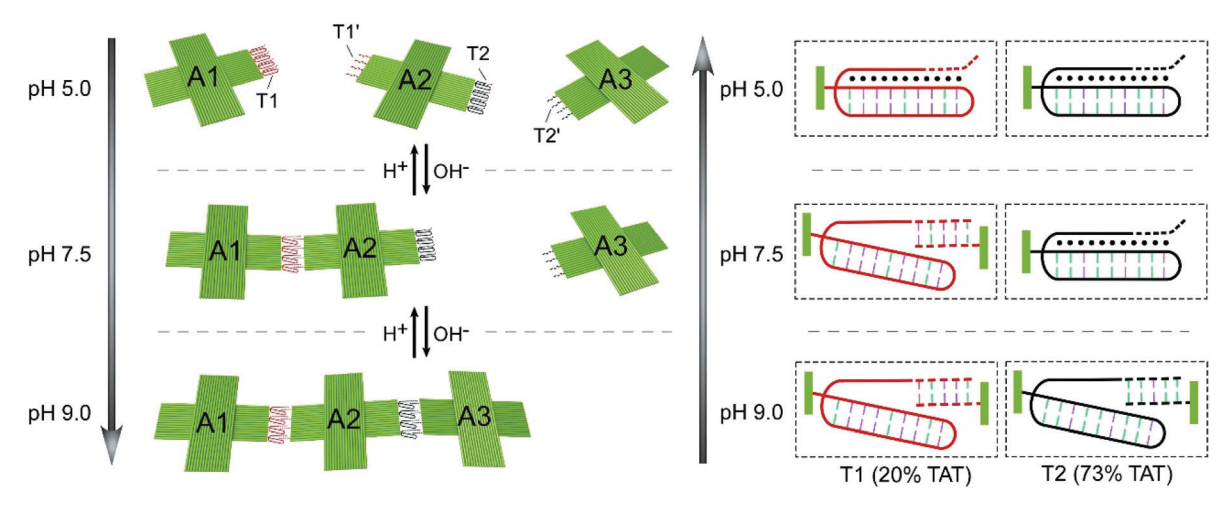


Fig. 1 Schematic drawing of the pH-stimulated stepwise assembly/disassembly of DNA origami trimer. The three-state transition of DNA origami (monomer-dimer-trimer) is triggered by the pH-dependent DNA triplexes in response to three different pH environments.

ssDNA domain of the DNA triplexes is available for complementary DNA hybridization, linking components together, while refolding the DNA triplex will disrupt this complementary pairing, and lead to dissociation of the components. Compared with the two-state transition of i-motif occurring within a narrow pH range, ^{18,28} DNA triplexes are more tunable for a wide range of pH response, thereby providing opportunities for multiple-step regulation. Here, we tested the selective assembly/disassembly of DNA origami trimers and more complex nine-unit DNA origami clusters, in a stepwise fashion, based on DNA triplexes in response to three different pH environments. The reversible control of the association/dissociation of the nanoclusters is demonstrated by AFM images and gel analysis.

Fig. 1 shows a schematic illustration of in situ stepwise assembly/disassembly of DNA origami trimers. Two different types of intramolecular DNA triplexes, which stimulate the proposed multi-state transitions of the DNA origami trimers, are involved. The right arm of tile A1 is modified with four strands of DNA triplex set (T1) containing 20% T-A·T, while the right arm of tile A2 is attached with four strands of DNA triplex set (T2) containing 73% T-A·T (triplex-to-duplex transition occurring at pH = \sim 7.5 and pH = \sim 9.0 respectively). ²⁶ Both types of DNA triplexes contain sticky ends (dashed line), which are complementary to the ssDNA overhangs, T1' and T2', decorated at the left arms of tiles A2 and A3, respectively. The prepared three DNA origami monomers (A1, A2, and A3) were mixed at a molar ratio of 1:1:1 in a 1× TAE buffer solution (pH = 5.0) containing 10 mM of magnesium acetate. At pH = 5.0, both T1 and T2 preferentially form intramolecular triplexes (folded state) and limit the cohesion ability of their sticky ends, thereby keeping DNA origami A1, A2, and A3 unhybridized in solution. As the pH value is increased from 5.0 to 7.5, DNA triplex sets T1 and T2 respond differently: T1 dissociates and, thus, releases the sticky ends on tile A1, which then bind to their complementary partners (T1') on tile A2. This results in the formation of A1/A2 dimers after thermal annealing from 35 °C to 25 °C over 12 h while, on the other hand, T2 still remains folded due to high T-A·T content (73%), leaving the tile A3 monomer alone. When the pH value is further increased to 9.0, A1/A2/A3 trimers can be formed through sticky-end association between dimer A1/A2 and tile A3, that results from the unfolding of DNA triplex T2 and, thereby, causes release of the sticky ends on tile A2. This assembly system can also be reconfigured in reverse via a decrease of pH back to neutral, and further to an acidic condition, allowing the origami trimers to dissociate into dimers and further into monomers, once again.

As proof-of-principle, the reversible assembly of two DNA origami dimers (A1/A2 and A2/A3), triggered by DNA triplex sets, T1 and T2, respectively, was first tested. In the case of A1/ A2 dimer, as shown in Fig. 2, at pH = 5.0, the hybridization between tile A1 and tile A2 is inhibited due to the strong stability of DNA triplex T1. In contrast, changing the pH to 7.5 causes the destabilization of Hoogsteen interactions in the

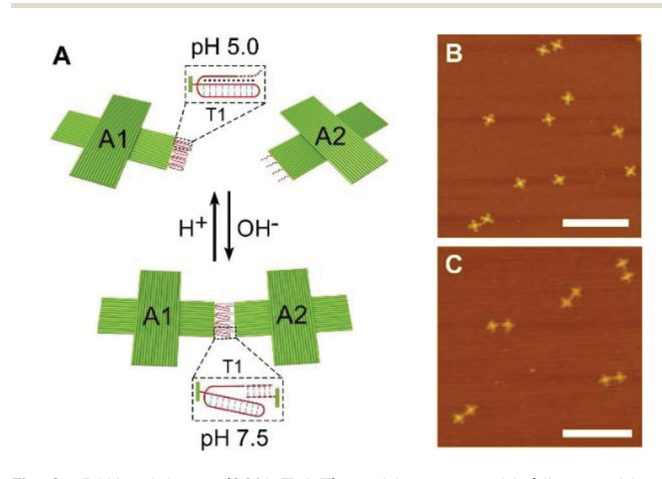


Fig. 2 DNA triplexes (20% T-A·T) - driven assembly/disassembly of DNA origami dimer A1/A2. (A) Schematic drawing of the pH-stimulated cyclic assembly of DNA origami dimers through DNA triplex set T1 between pH 5.0 and 7.5. (B) AFM images of DNA origami monomer at pH = 5.0 and dimer at pH = 7.5 (C). Scale bars: 500 nm.

Communication Nanoscale

DNA triplexes, thereby, triggering two origami monomers to associate into the dimer structures (A1/A2). Fig. 2B and C show the resulting origami monomers and dimers observed at pH 5.0 and pH 7.5, respectively. The statistical analysis of the atomic force microscopy (AFM) images reveals that ~87% DNA origami tiles are present in a dimeric form at pH 7.5 (see Fig. S1 and Table S1†). Similarly, the DNA triplex T2 guided reversible monomer – dimer transition of another origami pair, A2/A3, was also examined. The AFM image analysis, as shown in Fig. S2,† presents a reversible transition from the monomer tiles (at pH 7.5) to the dimers (A2/A3, at pH 9.0), with a ~86% of dimer formation yield (Table S2†). In order to increase the targeted dimer yield, the thermal annealing process was employed after the pH triggered unfolding of DNA triplexes. According to our agarose gel analysis, the annealing process enhances the dimer (A1/A2) yield from ~75% to ~89%, when the mixture of A1 and A2 is annealed from 38 °C to 25 °C, instead of incubating at room temperature for 6 h (Fig. S3†). However, for the dissociation process, the annealing procedure is not required because of the formation of stabilized DNA triplexes after changing the pH. 29-31 Together, these results confirm that the DNA triplex-assisted assembly of each DNA origami dimer works effectively in response to their corresponding pH environment.

Next, the reversible three-state transition (monomer-dimertrimer) of a three-tile origami system (A1, A2, and A3), regulated by the conformation change of DNA triplex sets T1 and T2 together, was investigated (Fig. 1). Fig. 3A-C show the representative AFM images of the resulting productions generated at pH = 5.0, 7.5, and 9.0, respectively. It can be seen that a majority of DNA origami tiles, at pH 5.0, remain as monomers. When the pH increases to 7.5, as expected, a mixture of dimers (A1/A2) and monomers (A3) yields. Upon further increase of pH to 9.0, linear origami trimer structures (A1/A2/ A3) start to appear (Fig. 3C and Fig. S4†). The cross-section analysis of DNA origami monomer, dimer, and trimer are shown in Fig. S5,† their corresponding sizes are consistent with our design. The stepwise reversible assembly process of DNA origami trimers is also demonstrated by gel electrophoresis. As can be seen in Fig. 3D, along with an increase in pH, from 5.0 to 7.5, and further to 9.0, the targeted bands exhibit a slower and slower electrophoretic mobility corresponding to the formation of dimers and trimers at pH 7.5 and 9.0, respectively. When reducing the pH back, from 9.0 to 7.5, and further to 5.0, the samples result in faster and faster electrophoretic mobility, indicating that the trimers undergo structural dissociation, thereby transitioning to dimers + monomers (A1/A2 + A3), and then further to monomers (A1, A2, and A3). Quantitative analysis of the gel band intensity shows that a majority of DNA tiles stay as monomers at pH 5.0; 55% origami tiles form dimers at pH 7.5; and 72% origami successfully assemble into trimers at pH 9.0. By switching the pH between 5, 7.5, and 9, the system can be further reconfigured multiple times in a fully reversible manner (Fig. S6†). These results suggest that the pH-regulated consecutive multistep assembly/disassembly of DNA nanostructures can be achieved by engineering the sequences of DNA triplexes.

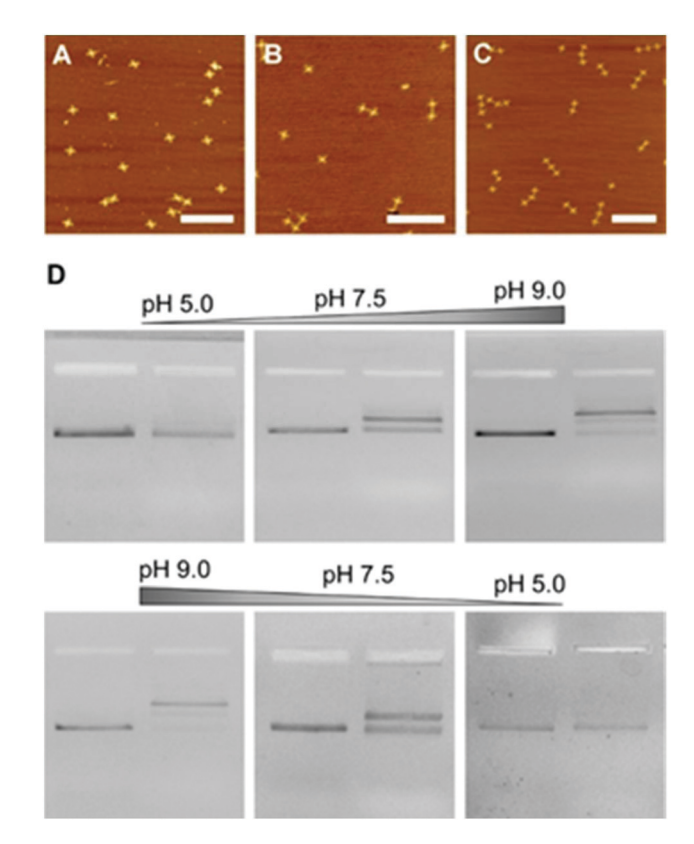


Fig. 3 pH-Stimulated stepwise assembly/disassembly of DNA origami trimer. (A-C) AFM images of DNA origami assemblies at pH = 5.0, 7.5, and 9.0, respectively, to show the three-state transitions from monomer to dimer to trimer. (D) Stepwise and reversible assembly of DNA origami trimer demonstrated by agarose gel electrophoresis. Left lane of each image is a DNA origami monomer used as reference control to show the band mobility of targeted dimers and trimers. Scale bars: 500 nm.

To further demonstrate the reversibility of pH-stimulated multiple steps of assembly of DNA origami nanostructures, the dynamic light scattering (DLS) method was used to monitor the assembly processes via detection of the size variations of DNA structures from monomers, dimers, to trimers in response to pH stimulation (Fig. S7 and S8†). Two working cycles composed of 9 steps of transition induced by pH changes between pH5 and pH 9 were observed (Fig. 4). In this way, the working system can be switched back and forth between the stepwise association and dissociation states controlled by pH stimulation. In addition, the DLS assay was also employed to monitor the dynamic dissociation of DNA origami nanostructures in real-time. After the pH was changed from 9 to 7.5, the size of DNA origami assemblies gradually decreased from ~75 nm to ~60 nm over the time course of 150 min (Fig. S9A†), indicating the DNA origami trimers were dissociated to dimers due to the release of tile A3 by refolding of DNA triplexes (73% T-A·T). Fig. S9B† shows the decreasing size of DNA origami assemblies from ~60 nm to ~50 nm once the pH further changed from 7.5 to 5, corresponding to the transition from dimers to monomers.

Encouraged by the successful assembly of the DNA origami trimers in a stepwise reversible manner, we further demonNanoscale Communication

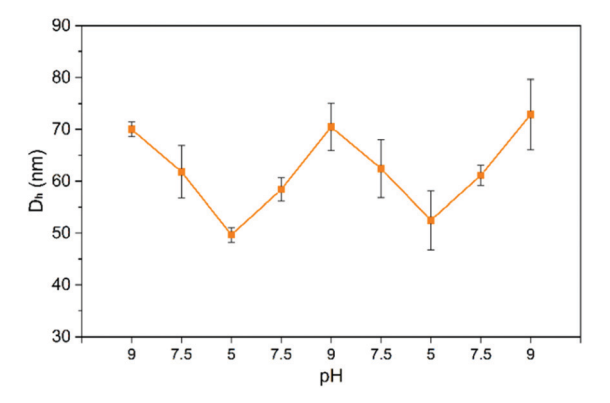


Fig. 4 Working cycles of DNA triplex-driven DNA origami nanostructures stepwise assembly/disassembly in response to pH stimulation. The size decreases after pH changing from 9 to 7.5, and keeps decreasing at pH = 5, then increases with pH increasing.

strate the scalability of the controlled formation of more complex 9-tile DNA nanoclusters, based on the same aforementioned approach, as schematically shown in Fig. 5A. In this design, three cross-shaped DNA origami tiles, A4 (blue), A5 (green), and A6 (brown), were employed. Each arm of tile A4 was modified with the four ssDNA (red), providing coupling to the complementary sticky-ends in the DNA triplex set T1* containing 20% T-A·T (red) decorated on one arm of tile A5. Two neighboring arms of tile A6 contain the two strands of DNA triplex set T2* with 73% T-A·T (black), whose sticky-end domains are complementary to the ssDNA (black) attached on the two arms of tile A5. In order to prevent the uncontrolled orientation of origami tiles, distinct sequences of hybridized

sticky-ends are designed in a prescribed order (see ESI† for DNA sequences). As demonstrated in previous studies, at pH 5, both DNA triplex sets T1* and T2* are in close states, thereby keeping all of the DNA origami in monomers. Increasing the pH to 7.5 leads to the dissociation of triplex set T1* and, thus, resulting in the appearance of 5-tile origami clusters. As the pH is further increased to pH 9.0, the triplex set T2* on tile A6 is also activated, leading to the formation of 9-tile nanoclusters. Fig. 5B-D, respectively, show the AFM images of resultant assemblies generated at pH 5.0, pH 7.5, and pH 9.0 after gel purification, which are in excellent agreement with our design (Fig. S10†). The gel mobility shift assay also confirms that this pH-induced stepwise assembly process is fully reversible (Fig. S11†). Due to the flexibility of a cross-shaped DNA origami unit and the incomplete transition of DNA triplexes from triplex-to-duplex states, the partial formation and aggregates of 5-tile and 9-tile clusters can be observed in the absence of previous gel purification, as evidenced by AFM images in Fig. S12.† Therefore, optimizing the structural rigidity of DNA units, and improving the pH sensitivity of DNA triplexes, or introducing other robust, and novel dynamic linkers into the system are the key to the scale-up of stepwise selfassembled DNA nanostructures.

Conclusions

We successfully demonstrate a pH-driven stepwise assembly/ disassembly of DNA origami nanoclusters with well-defined geometries for each step. Specifically, two types of DNA triplexes, containing 20% and 73% T-A·T, are utilized as the

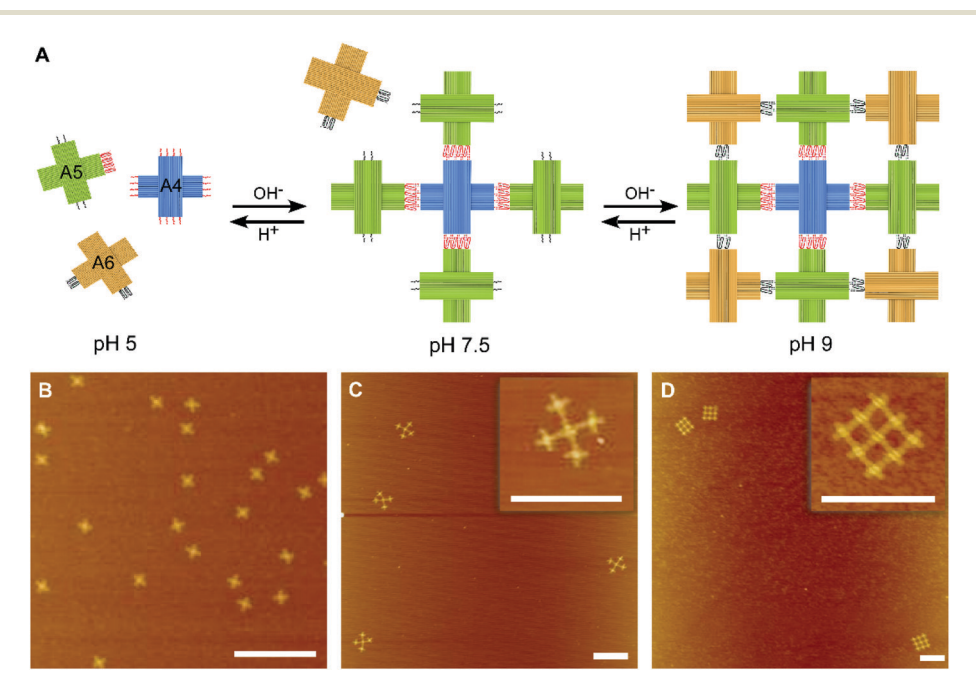


Fig. 5 pH-Trigged stepwise assembly/disassembly of 9-tile DNA origami nanoclusters. (A) Schematic drawings of the reversible association of 9-tile DNA origami clusters. (B-D) AFM images of DNA origami at pH = 5 (monomer), pH = 7.5 (5-tile), and pH = 9 (9-title), respectively. Scale bars: 500 nm.

Communication Nanoscale

dynamic bridges in controlling the reversible assembly of DNA clusters in response to successive pH-stimulation processes. We show the formation of DNA origami trimers and more complex 9-tile clusters in a stepwise, selective and reversible manner. Our study provides a new and straightforward approach for fabricating well-defined DNA nanostructures regulated by changes in pH value. These multi-level and dynamic assemblies, in particular, may attract biomedical applications due to their specific responses towards wide ranges of pH environments, 32,33 mimicking the different parts of organelles, for developing pH-responsive drug delivery,34 gene therapy, 35 and the enzyme cascade reactions. 36 Due to the competition of DNA triplexes at wide range of pH environments, it's also possible to use such structures for DNA computation.³⁷ Additionally, it is expected that other triggers, such as light, gas, ions, and ligands can be involved to mimic living organisms that can extend our capabilities to create more sophisticated and smart functional nanostructures.

Conflicts of interest

There are no conflicts to declare.

Acknowledgements

This work was supported by the National Science Foundation under grants CCF-1814797. R. Wang thanks Dr William Shih for his valuable suggestions.

References

- 1 Y. Bai, Q. Luo and J. Liu, Chem. Soc. Rev., 2016, 45, 2756-2767.
- 2 B. P. Glover and C. S. McHenry, Cell, 2001, 105, 925-934.
- 3 E. Winfree, F. R. Liu, L. A. Wenzler and N. C. Seeman, *Nature*, 1998, **394**, 539–544.
- 4 D. R. Han, S. Pal, Y. Yang, S. X. Jiang, J. Nangreave, Y. Liu and H. Yan, *Science*, 2013, 339, 1412–1415.
- 5 W. Y. Liu, H. Zhong, R. S. Wang and N. C. Seeman, *Angew. Chem., Int. Ed.*, 2011, **50**, 264–267.
- 6 P. Wang, S. Gaitanaros, S. Lee, M. Bathe, W. M. Shih and Y. Ke, *J. Am. Chem. Soc.*, 2016, **138**, 7733–7740.
- 7 J. Zheng, J. J. Birktoft, Y. Chen, T. Wang, R. Sha, P. E. Constantinou, S. L. Ginell, C. Mao and N. C. Seeman, *Nature*, 2009, 461, 74–77.
- 8 S. M. Douglas, H. Dietz, T. Liedl, B. Hogberg, F. Graf and W. M. Shih, *Nature*, 2009, **459**, 414–418.
- 9 D. R. Han, S. Pal, J. Nangreave, Z. T. Deng, Y. Liu and H. Yan, *Science*, 2011, 332, 342–346.
- 10 C. J. Serpell, T. G. Edwardson, P. Chidchob, K. M. Carneiro and H. F. Sleiman, J. Am. Chem. Soc., 2014, 136, 15767–15774.

- 11 Y. G. Ke, L. L. Ong, W. Sun, J. Song, M. D. Dong, W. M. Shih and P. Yin, *Nat. Chem.*, 2014, 6, 994–1002.
- 12 E. Benson, A. Mohammed, J. Gardell, S. Masich, E. Czeizler, P. Orponen and B. Hogberg, *Nature*, 2015, **523**, 441–444.
- 13 E. Kopperger, J. List, S. Madhira, F. Rothfischer, D. C. Lamb and F. C. Simmel, *Science*, 2018, 359, 296–301.
- 14 A. E. Marras, L. Zhou, H. J. Su and C. E. Castro, *Proc. Natl. Acad. Sci. U. S. A.*, 2015, 112, 713–718.
- 15 J. Song, Z. Li, P. Wang, T. Meyer, C. Mao and Y. Ke, *Science*, 2017, 357, eaan3377.
- 16 Z. Shi, C. E. Castro and G. Arya, ACS Nano, 2017, 11, 4617–4630.
- 17 Y. Yang, M. Endo, K. Hidaka and H. Sugiyama, *J. Am. Chem. Soc.*, 2012, 134, 20645–20653.
- 18 N. Wu and I. Willner, Nano Lett., 2016, 16, 6650-6655.
- 19 L. N. Green, A. Amodio, H. K. K. Subramanian, F. Ricci and E. Franco, *Nano Lett.*, 2017, 17, 7283–7288.
- 20 J. Wang, Z. Zhou, L. Yue, S. Wang and I. Willner, *Nano Lett.*, 2018, 18, 2718–2724.
- 21 S. Yang, W. Liu, R. Nixon and R. Wang, *Nanoscale*, 2018, 10, 3626–3630.
- 22 N. Wu and I. Willner, Nano Lett., 2016, 16, 2867-2872.
- 23 N. Wu and I. Willner, Nanoscale, 2017, 9, 1416-1422.
- 24 Y. Hu, A. Cecconello, A. Idili, F. Ricci and I. Willner, *Angew. Chem., Int. Ed.*, 2017, **56**, 15210–15233.
- 25 J. Wang, L. Yue, S. Wang and I. Willner, *ACS Nano*, 2018, **12**, 12324–12336.
- 26 S. Rhee, Z. Han, K. Liu, H. T. Miles and D. R. Davies, *Biochemistry*, 1999, 38, 16810–16815.
- 27 A. Idili, A. Vallee-Belisle and F. Ricci, J. Am. Chem. Soc., 2014, 136, 5836–5839.
- 28 L. Heinen and A. Walther, Chem. Sci., 2017, 8, 4100-4107.
- 29 J. Volker, S. E. Osborne, G. D. Glick and K. J. Breslauer, *Biochemistry*, 1997, **36**, 756–767.
- 30 M. S. Searle and D. H. Williams, *Nucleic Acids Res.*, 1993, 21, 2051–2056.
- 31 G. E. Plum, Y. W. Park, S. F. Singleton, P. B. Dervan and K. J. Breslauer, *Proc. Natl. Acad. Sci. U. S. A.*, 1990, 87, 9436– 9440
- 32 S. Mura, J. Nicolas and P. Couvreur, *Nat. Mater.*, 2013, 12, 991–1003.
- 33 F. Muhammad, M. Guo, W. Qi, F. Sun, A. Wang, Y. Guo and G. Zhu, J. Am. Chem. Soc., 2011, 133, 8778–8781.
- 34 Y. Dong, Z. Yang and D. Liu, Acc. Chem. Res., 2014, 47, 1853–1860.
- 35 A. Bacolla, G. Wang and K. M. Vasquez, *PLoS Genet.*, 2015, **e1005696**, 1–12.
- 36 V. Linko, M. Eerikainen and M. A. Kostiainen, *ChemComm*, 2015, **51**, 5351–5354.
- 37 G. Seelig, D. Soloveichik, D. Y. Zhang and E. Winfree, *Science*, 2006, 314, 1585–1588.